arXiv:0709.1652v1 [hep-ph] 11 Sep 2007

Top Quarks, Axigluons and Charge Asymmetries at Hadron Colliders

Oscar Antuñano [(a)][*], **Johann H. Kühn** [(b)][†], **Germán Rodrigo** [(a)][‡]

[(a)] Instituto de Física Corpuscular, CSIC-Universitat de València,
Apartado de Correos 22085, E-46071 Valencia, Spain.

[(b)] Institut für Theoretische Teilchenphysik, Universität Karlsruhe, D-76128 Karlsruhe, Germany.

Abstract

Axigluons are colored heavy neutral gauge boson that couple to quarks through an axial vector current and the same strong coupling as gluons. The most important model-independent manifestation of axigluons is the generation of a forward–backward asymmetry in top-antitop quark production at $p\bar{p}$ collisions which originates from the charge asymmetry. We update our previous analysis for the inclusive QCD induced forward–backward asymmetry and define a new observable which is more sensitive to the effect than the forward–backward asymmetry. Furthermore, we find a lower limit of 1.2 TeV at 90% C.L. on the axigluon mass from recent measurements of the asymmetry at Tevatron. Also at LHC, the charge asymmetry is sizable in suitably selected samples. We evaluate this asymmetry in the central region for different selection cuts and show that, like at Tevatron, the charge asymmetry can probe larger values of the axigluon mass than the dijet mass distribution.

[*]E-mail: oscant@ific.uv.es
[†]E-mail: johann.kuehn@uni-karlsruhe.de
[‡]E-mail: german.rodrigo@ific.uv.es

1 Introduction

The Large Hadron Collider (LHC) will enter into operation very soon, allowing to explore the existence of new physics at the TeV energy scale with unprecedented huge statistics [1]. Since the top quark is the heaviest known elementary particle it plays a fundamental role in many extensions of the Standard Model (SM), and its production and decay channels are promising probes of new physics. The total cross section of top-antitop quark production at LHC is about 100 times larger than at Tevatron. This will lead to the production of millions of $t\bar{t}$ pairs per year even at the initial low luminosity of $\mathcal{L} = 10^{33} \text{cm}^{-2}\text{s}^{-1}$ (equivalent to 10 fb^{-1}/year integrated luminosity).

Some properties of the top quark can be studied at Tevatron through the forward–backward asymmetry which originates from the charge asymmetry [2, 3]. The Born processes relevant for top quark production, $q\bar{q} \to t\bar{t}$ and $gg \to t\bar{t}$, do not discriminate between final quark and antiquark, thus predicting identical differential distributions also for the hadronic production process. At order α_s^3 however a charge asymmetry is generated and the differential distributions of top quarks and antiquarks are no longer equal. A similar effect leads also to a strange-antistrange quark asymmetry, $s(x) \neq \bar{s}(x)$, through next-to-next-to-leading (NNLO) evolution of parton densities [4]. The inclusive charge asymmetry has its origin in two different reactions: radiative corrections to quark-antiquark annihilation (Fig. 1) and interference between different amplitudes contributing to gluon-quark scattering $qg \to t\bar{t}q$ and $\bar{q}g \to t\bar{t}\bar{q}$. Gluon-gluon fusion remains obviously symmetric. The integrated forward–backward asymmetry has been predicted to be about $+5\%$ at Tevatron [2]; i.e. top quarks are preferentially emitted in the direction of the incoming protons. This prediction suffers, however, from a sizable uncertainty because, although arising from a one-loop calculation and the corresponding real emission terms, it is still a leading order (LO) result. At LHC the total forward–backward asymmetry vanishes trivially because the proton-proton initial state is symmetric. A charge asymmetry is, however, still visible in suitably defined distributions [2].

In $t\bar{t}$ plus jet production, which represents an important background process for Higgs boson searches in electroweak vector boson fusion and $t\bar{t}H$ production, the asymmetry, of order α_s^3, is a tree-level effect [3] with sign opposite to the one given for inclusive production [2]. The next-to-leading (NLO) order QCD corrections to the $t\bar{t}$+jet exclusive channel have become available very recently [5], providing a NLO prediction for the charge asymmetry. At Tevatron the exclusive forward–backward asymmetry of top quarks is drastically reduced at NLO, from about -7% at LO to $-1.5 \pm 1.5\%$, where the large uncertainty is due to the residual scale dependence. A priori one can not extrapolate this unexpected result to the totally inclusive asymmetry. Already at LO the size of the asymmetry in the $t\bar{t}$+jet event sample depends on the jet resolution parameters, and on the softness of the radiated gluon. A smaller minimal gluon energy generates a larger negative asymmetry, and vice versa, and the size of NLO corrections might be different for different jet setups. Furthermore, because the one-loop corrections to the inclusive asymmetry are positive and larger than the negative contribution of real gluon bremsstrahlung a smaller prediction for the asymmetry in the $t\bar{t}$+jet sample might give rise to a larger inclusive asymmetry. Unfortunately, the only way to obtain a more accurate prediction for the inclusive asymmetry is to evaluate the higher order corrections corresponding to a difficult two-loop calculation.

The forward–backward asymmetry of top quarks has already attracted much experimental interest at Tevatron. A detailed study of the feasibility of the measurement in the dilepton and lepton+jet channels has been presented in Ref. [6]. Experimental measurements have already been performed in Refs. [7, 8, 9]. In Ref. [9], based on 695 pb^{-1} integrated luminosity, the forward–backward asymmetry in the lepton

plus jets channels was found to be

$$A_{\mathrm{FB}} = 0.20 \pm 0.11 \text{ (stat)} \pm 0.047 \text{ (sys)} . \tag{1}$$

A very similar result was obtained for the inclusive asymmetry in Refs. [7, 8] based on 955 pb^{-1} integrated luminosity, and again in the lepton plus jets channels:

$$A(\Delta y \cdot Q_l) = 0.23 \pm 0.12 \text{ (stat)} \pm {}^{0.056}_{0.057} \text{ (sys)} , \tag{2}$$

where the charge asymmetry is defined by the difference in the number of events with positive and negative $\Delta y \cdot Q_l$, the rapidity difference of the semileptonically and hadronically decaying top quark times the charge of the charged lepton. They also have measured the exclusive asymmetry of the four- and five-jet samples:

$$\begin{aligned} A^{4\mathrm{j}}(\Delta y \cdot Q_l) &= 0.11 \pm 0.14 \text{ (stat)} \pm {}^{0.036}_{0.034} \text{ (sys)} . \\ A^{5\mathrm{j}}(\Delta y \cdot Q_l) &= 0.37 \pm 0.30 \text{ (stat)} \pm {}^{0.075}_{0.066} \text{ (sys)} . \end{aligned} \tag{3}$$

The asymmetry in the five-jet sample although expected to be negative is statistically limited, and the comparison with the NLO prediction [5] would require the use of the same jet definition. The inclusive asymmetry in both experimental analyses, although compatible with the theoretical prediction, is still statistically dominated. The statistical error, however, is expected to be reduced to 0.04 with 8 fb^{-1} [9], which is comparable with the systematic error.

With these results at hand one might try to test new physics beyond the SM. The production of $t\bar{t}$ through a colored heavy neutral gauge boson will manifest itself through a bump in the invariant mass distribution of the top-antitop quark pair [10, 11, 12], and in some models might give rise to a sizable forward–backward asymmetry [13]. Models which extend the standard color gauge group to $SU(3)_L \times SU(3)_R$ at high energies, the so called chiral color theories [10], predict the existence of a massive, color-octet gauge boson, the axigluon, which couples to quarks with an axial vector structure and the same strong interaction coupling strength as QCD. Although there are many different implementations of chiral color theories with new particles in varying representations of the gauge groups, the most important model-independent prediction of these models is the existence of the axigluon. Similar states are also predicted in technicolor models [14]. The main signature is the appearance of a charge asymmetry of order α_s^2. Because the coupling of the axigluon to quarks is an axial vector coupling the charge asymmetry that can be generated is maximal.

Axigluon masses below 1 TeV are already ruled out. The Tevatron searches for new resonances decaying to dijets [15, 16] exclude the mass range $200 < m_A < 1130$ GeV at 95% C.L. Lighter axigluons, with masses lower than 50 GeV, were excluded studying Z decays, where the axigluon is produced by the bremsstrahlung of the quarks [17], and also studying the decay of Upsilon [18] and the Z decay to a gluon and an axigluon [19]. The intermediate mass range window has also been excluded [20].

In this paper we shall update our prediction for the inclusive forward–backward asymmetry at Tevatron, and propose a new differential distribution that enhances the asymmetry by almost a factor 1.5. We then obtain a new constraint on the axigluon mass from the actual measurement of the inclusive asymmetry at Tevatron. Finally, we show that at LHC the study of the differential charge asymmetry is sensitive to larger axigluon masses than the top-antitop invariant mass distribution.

2 The QCD induced charge asymmetry

The QCD induced charge asymmetry in the reaction $q\bar{q} \to t\bar{t}(g)$ is generated by the interference of final-state with initial-state gluon radiation [Fig. 1, (a)×(b)] and by the interference of virtual box diagrams with the Born process [Fig. 1, (c)×(d)]. The asymmetric contribution of the virtual corrections exhibit soft singularities that are canceled by the real contribution, but do not exhibit collinear light quark mass singularities which would have to be absorbed by the lowest order process which however is symmetric. Ultraviolet divergences are absent for the same reason. The virtual plus soft radiation on one hand and the real hard radiation on the other contribute with opposite signs, with the former always larger that the latter such that the inclusive asymmetry becomes positive. Top quarks are thus preferentially emitted in the direction of the incoming quark at the partonic level, which translates to a preference in the direction of the incoming proton in $p\bar{p}$ collisions. Flavour excitation $gq(\bar{q}) \to t\bar{t}X$ generates already at tree-level a forward–backward asymmetry which at Tevatron is also positive although one order of magnitude smaller than the asymmetry from $q\bar{q}$ annihilation.
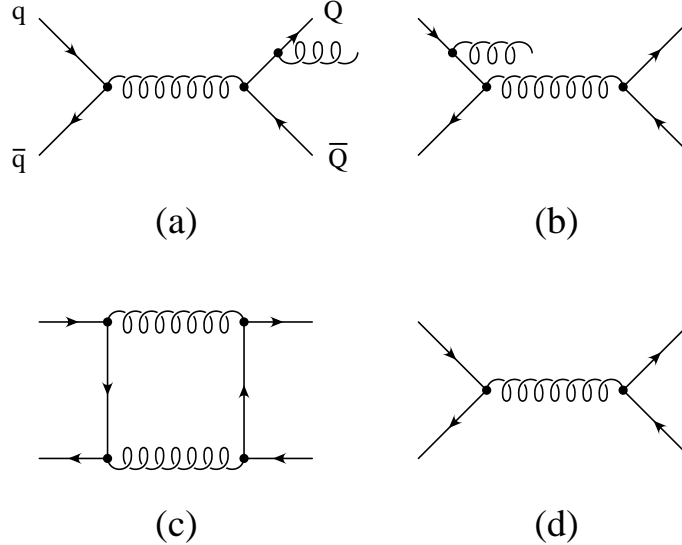

Figure 1: Origin of the QCD charge asymmetry in hadroproduction of heavy quarks: interference of final-state (a) with initial-state (b) gluon bremsstrahlung, plus interference of the double virtual gluon exchange (c) with the Born diagram (d). Only representative diagrams are shown.

The differential charge asymmetry of the single quark rapidity distribution is defined through

$$A(y) = \frac{N_t(y) - N_{\bar{t}}(y)}{N_t(y) + N_{\bar{t}}(y)} , \qquad (4)$$

where y denotes the rapidity of the top (antitop) quark in the laboratory frame and $N(y) = d\sigma/dy$. Since $N_{\bar{t}}(y) = N_t(-y)$ as a consequence of charge conjugation symmetry, $A(y)$ can also be interpreted as a forward–backward asymmetry of the top quark. We have updated our previous analysis [2] by using the new value of the top quark mass, $m_t = 170.9 \pm 1.1\,(\text{stat}) \pm 1.5\,(\text{sys})$ GeV [21], and the new set of MSRT2004 [22] structure functions. For the total charge asymmetry at $\sqrt{s} = 1.96$ TeV we predict

$$A = \frac{N_t(y \geq 0) - N_{\bar{t}}(y \geq 0)}{N_t(y \geq 0) + N_{\bar{t}}(y \geq 0)} = 0.051(6) , \qquad (5)$$
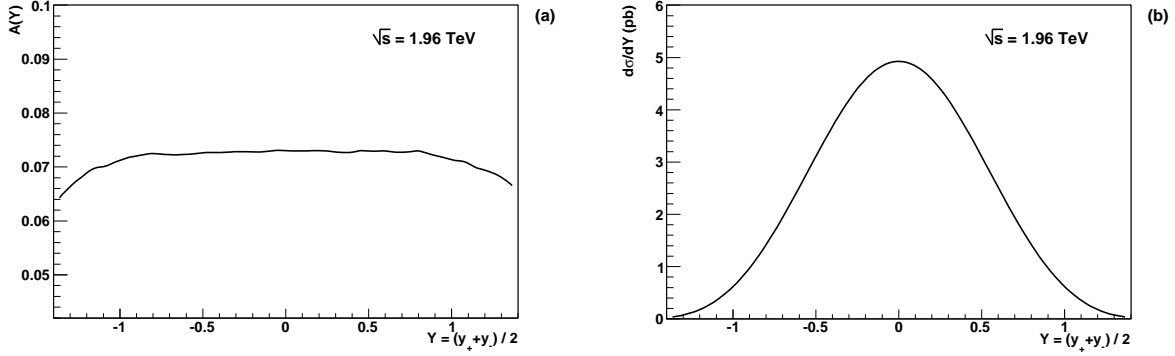
3

Figure 2: (a) Differential QCD asymmetry in the average rapidity at Tevatron, $\sqrt{s} = 1.96$ TeV. (b) Average rapidity differential distribution. Factorization and renormalization scales are set to $\mu = m_t$.

where different choices of the parton distribution functions, and different choices of the factorization and renormalization scales, $\mu = m_t/2$ and $\mu = 2m_t$, and a variation of the top mass within the experimental error have been considered. We have also included the contribution of the mixed QCD-electroweak interference that leads to an increase of the asymmetry as given by QCD by a factor 1.09 [2]. The result is close to our earlier prediction: $A = 4.8 - 5.8\%$ [2]. Both the numerator and denominator are evaluated in LO. NLO corrections to the total $t\bar{t}$ production cross section are known to be large, around 30% or even larger [23]. Applying a K-factor of 1.3 to the denominator would reduce the asymmetry to $A = 0.036(4)$. In the absence of NLO corrections to the numerator we nevertheless stay with the LO approximation in both numerator and denominator, expecting the dominant corrections from collinear emission to cancel. From a more conservative point of view an uncertainty of around 30% has to be assigned to the prediction of the asymmetry.

Let us now consider events where the rapidities y_+ and y_- of both the top and antitop quarks have been determined, and define a new differential distribution that leads to an enhancement of the charge asymmetry. We define

$$Y = \frac{1}{2}(y_+ + y_-) \,, \tag{6}$$

as average rapidity. Then, we consider the differential pair asymmetry $\mathcal{A}(Y)$ for all events with fixed Y as a function of Y:

$$\mathcal{A}(Y) = \frac{N_{\text{ev.}}(y_+ > y_-) - N_{\text{ev.}}(y_+ < y_-)}{N_{\text{ev.}}(y_+ > y_-) + N_{\text{ev.}}(y_+ < y_-)} \,. \tag{7}$$

In Figure 2(a) we show the differential pair asymmetry $\mathcal{A}(Y)$ versus the average rapidity for the Tevatron. The renormalization and factorization scales are set to $\mu = m_t$, and we use the LO MSRT2004 [22] parton distributions with three fixed flavours. Asymmetric contributions from flavour excitation processes, i.e. from $gq(g\bar{q})$ collisions, are negligible. We obtain an almost flat positive asymmetry of the order of 7%. For reference, we also plot in Figure 2(b) the differential cross section as function of the average rapidity. For the integrated pair asymmetry we find

$$\mathcal{A} = \frac{\int dY (N_{\text{ev.}}(y_+ > y_-) - N_{\text{ev.}}(y_+ < y_-))}{\int dY (N_{\text{ev.}}(y_+ > y_-) + N_{\text{ev.}}(y_+ < y_-))} = 0.078(9) \,, \tag{8}$$

4

where the error has been estimated as for the forward–backward asymmetry. Numerator and denominator are evaluated in leading order.

The integrated pair asymmetry is equivalent to the definition of the asymmetry used in Refs. [7, 8]. The reason for the enhancement of the effect can be understood as follows: by defining the pair asymmetry one essentially investigates the forward–backward asymmetry in the $t\bar{t}$ rest frame, where the forward–backward asymmetry amounts to $7 - 8.5\%$ [2], depending on $\hat{s}$. This value is largely recovered by considering the pair asymmetry $\mathcal{A}(Y)$, independently of Y. In contrast events where both t and $\bar{t}$ are produced with positive and negative rapidities do not contribute to the integrated forward–backward asymmetry A, which is therefore reduced to around 5%.

3   Axigluon limits from Tevatron

The interference between the gluon and axigluon induced amplitudes respectively for the reaction $q\bar{q} \rightarrow t\bar{t}$ does not contribute to the production cross section. However, it generates a charge asymmetry that gives rise to a forward–backward asymmetry in $p\bar{p}$ collisions in the laboratory frame [13]. The square of the axigluon amplitude is symmetric and contributes to the total cross-section, which will show a typical resonance peak in the top-antitop invariant mass distribution [11, 12]. While the interference term is suppressed by the squared axigluon mass $1/m_A^2$, the contribution of the square of the axigluon amplitude will be suppressed by $1/m_A^4$. It is therefore obvious that the forward–backward asymmetry is potentially sensitive to larger values of the axigluon mass than the top-antitop dijet distribution . Gluon-gluon fusion is not affected by the axigluon exchange because there are no direct gluon-axigluon vertices with an odd number of axigluons [11] due to parity. The expressions that we use for the partonic Born cross-section are summarized in Appendix A.
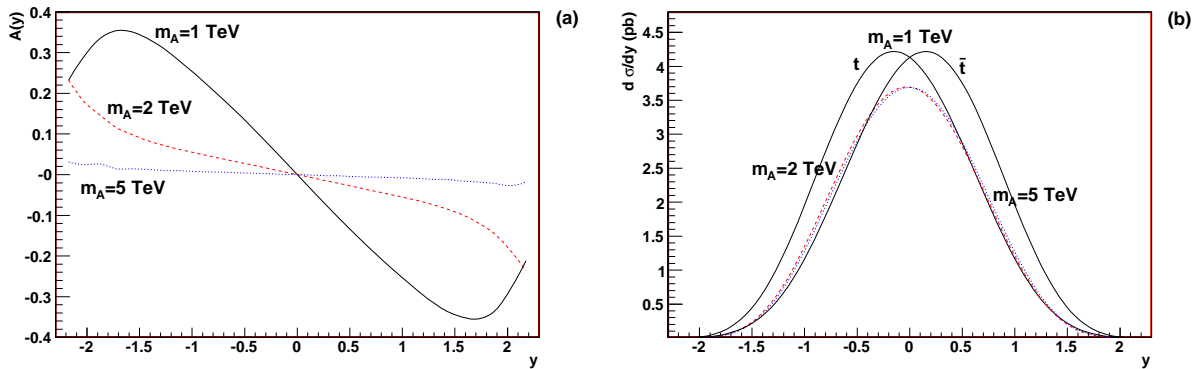

Figure 3: (a) Differential top quark charge asymmetry in $p\bar{p}$ collisions at Tevatron, $\sqrt{s} = 1.96$ TeV, for different values of the axigluon mass. (b) Rapidity distribution of top and antitop quarks for $m_A = 1$ TeV. For $m_A = 2$ TeV (dashed) and 5 TeV (dotted) we only represent the top quark distribution. Factorization and renormalization scales are set to $\mu = m_t$.

The interference between the amplitudes for production of $t\bar{t}$ through a gluon and an axigluon, respectively, vanishes upon integration over any charge symmetric part of the phase space and thus does not contribute to the production cross-section. However, the charge asymmetry resulting from this in-
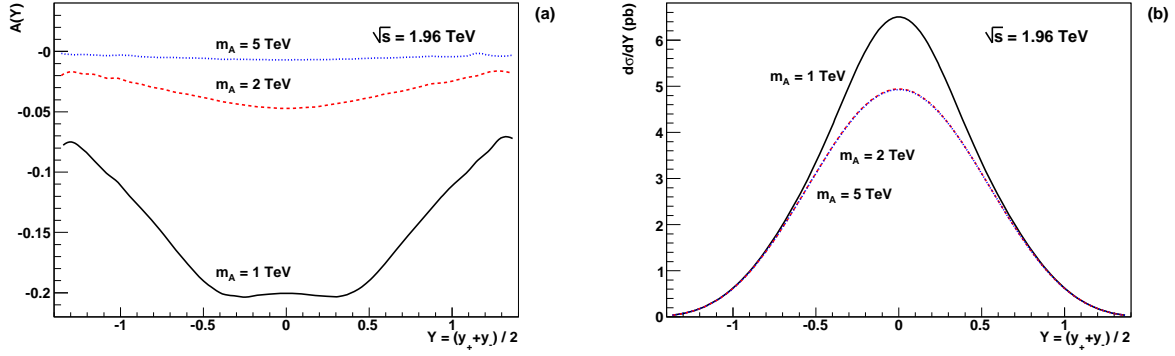
Figure 4: (a) Differential pair asymmetry in $p\bar{p}$ collisions at Tevatron, $\sqrt{s} = 1.96$ TeV, for different values of the axigluon mass. (b) Corresponding differential cross section $d\sigma/dY$. Factorization and renormalization scales are set to $\mu = m_t$.

	QCD	$m_A = 1\,\mathrm{TeV}$	$m_A = 2\,\mathrm{TeV}$	$m_A = 5\,\mathrm{TeV}$
$A_{\mathrm{FB}} = A$	$0.051(6)$	$-0.133(9)$	$-0.027(2)$	$-0.0041(3)$
$\mathcal{A}$	$0.078(9)$	$-0.181(11)$	$-0.038(3)$	$-0.0058(4)$

Table 1: Forward–backward and pair asymmetries at Tevatron, $\sqrt{s} = 1.96$ TeV, for different values of the axigluon mass.

terference may well be more sensitive to the existence of axigluons than the contribution of the squared amplitude, in particular in the case of large m_A, and will, furthermore, be a characteristic consequence of its axial nature.

In Fig. 3(a) the differential charge asymmetry $A(y)$ at the Tevatron is shown for different values of the axigluon mass as a function of the top quark rapidity. The QCD induced piece is not included in this figure. In Fig. 3(b) the top and antitop quark rapidity distributions are shown, again at LO, for $m_A = 1$ TeV (for larger values of the axigluon mass we only plot the top quark distribution). Due to the axigluon contribution the top quark distribution is shifted to negative values of the rapidity while the antitop quark distribution prefers positive values. The corresponding curves for the pair asymmetry $\mathcal{A}(Y)$ are shown in Fig. 4(a), the differential pair cross section $d\sigma/dY$ in Fig. 4(b). In Table 1 we present the prediction for the integrated forward–backward asymmetry for different values of the axigluon mass. We also give values for the integrated pair asymmetry $\mathcal{A}$ as defined in Eq. (8). The uncertainty of the predictions is estimated as before. The size of the pair asymmetry is larger than the forward–backward asymmetry. The enhancement factor is however somewhat smaller than in QCD.

As explained in the introduction, the forward–backward asymmetry A_{FB} and the integrated pair asymmetry have already been measured at the Tevatron [7, 8, 9]. The uncertainty of these preliminary results is still very large, and statistically dominated. The different experimental analyses are based on the same data sample and give a very similar result for the inclusive asymmetry. The subsequent discussion is thus of qualitative nature only. In Fig. 5(a) and 5(b) we compare the experimental measurements, with the SM contribution subtracted (Eq. (5) and Eq. (8) respectively), to the asymmetry generated by the axigluon. At the two sigma level axigluon masses below $m_A = 1.2$ GeV are excluded. Both asym-
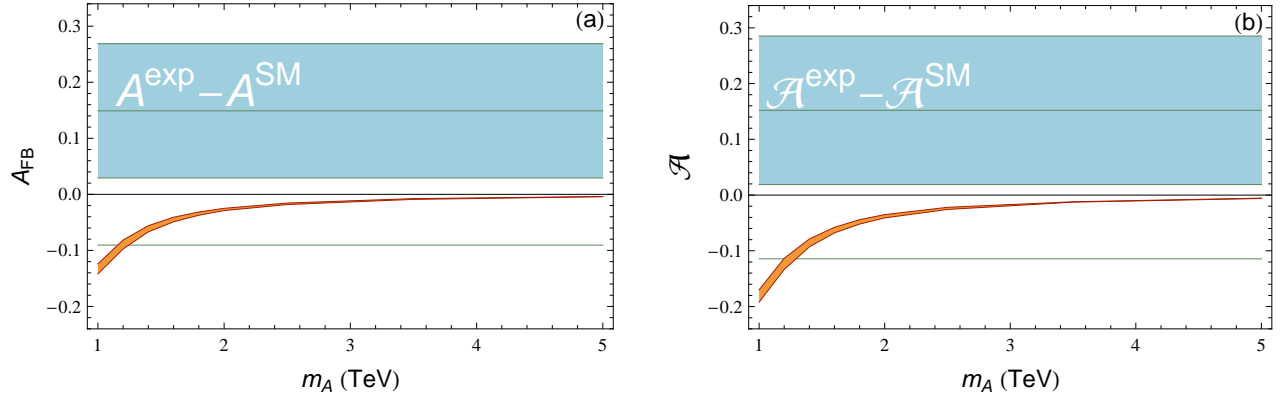
Figure 5: Comparison of the top quark forward–backward (a) and pair (b) asymmetry generated by the exchange of a massive axigluon to the experimental measurement at Tevatron once the theoretical prediction in the SM is subtracted. The 2σ contour is also showed.

metries give a very similar lower bound. It is clear that a more accurate experimental measurement and theoretical prediction will allow to further constrain the axigluon mass. However, at present the largest uncertainty by far is of experimental origin, and it will be reduced with more statistics. In this case, we will be in the interesting situation where axigluon masses that are not accessible at Tevatron through the study of the dijet cross-section can be excluded by the forward–backward or the pair asymmetries.

4 QCD and axigluon induced asymmetries at the LHC

Top quark production at LHC is forward–backward symmetric in the laboratory frame as a consequence of the symmetric colliding proton-proton initial state. Furthermore, the total cross section is dominated by gluon-gluon fusion and thus the charge asymmetry generated from the $q\bar{q}$ and gq ($g\bar{q}$) reactions is negligible in most of the kinematic phase-space. The effect can be studied nevertheless by selecting appropriately chosen kinematic regions. At LHC the QCD asymmetry predicts a slight preference for centrally produced antitop quarks, with top quarks more abundant at very large positive and negative rapidities [2]. The charge asymmetry as defined in Eq. (4) is, however, only sizable in regions with low event rates and large rapidities, where the experimental observation might be difficult. In Fig. 6(a) we present the differential charge asymmetry generated by the exchange of an axigluon as a function of rapidity, choosing $m_A = 1, 2$ and 5 TeV. We observe a similar behaviour as predicted by QCD but with the opposite sign; top quarks are slightly more abundant in the central region, while a sizable negative asymmetry is found at large values of the rapidity. For $m_A = 5$ TeV the asymmetry is almost negligible throughout, a consequence of the relatively small $t\bar{t}$ mass and the correspondingly strong suppression of the axigluon amplitude.

We shall therefore analyze the effect of selecting samples with high invariant masses of the top-antitop quark pair. Those samples should have a higher amount of $q\bar{q}$ induced events, and furthermore, an enhanced axigluon amplitude even for large m_A. Thus a sizable asymmetry is expected, although at the price of reducing the total event rate. This should not be a problem at LHC due to the huge top-antitop quark yields. In Fig. 7(a) we show the differential charge asymmetry generated by axigluons of mass $m_A = 1$ TeV for samples with invariant masses larger than $1, 2$ and 3 TeV respectively. A large
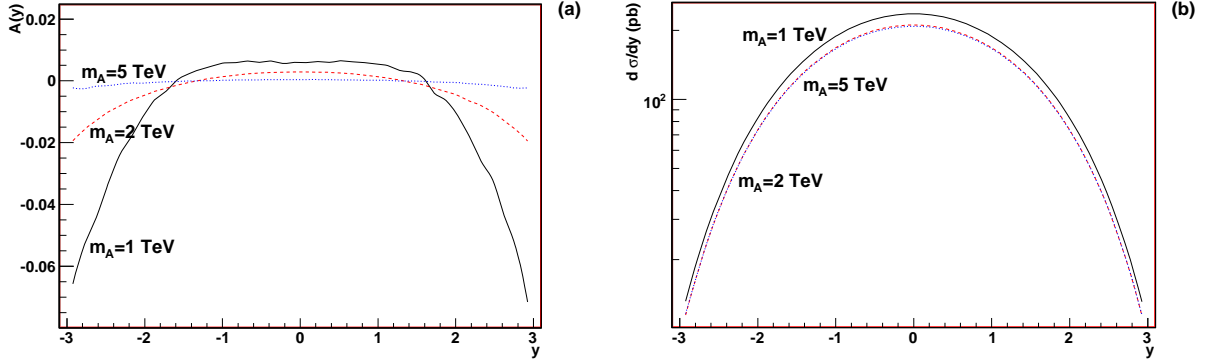
Figure 6: (a) Differential top quark charge asymmetry in pp collisions at LHC, $\sqrt{s} = 14$ TeV, for different values of the axigluon mass. (b) Rapidity distribution of top quarks for different values of the axigluon mass. Factorization and renormalization scales are set to $\mu = m_t$.

asymmetry with a maximum in the central region ranging from -8% to -30% is predicted. In Fig. 7(b) we show the corresponding top and antitop quark rapidity distributions. The total single inclusive cross sections are equal but the rapidity distributions are not, with antitop quarks more abundant in the central region. Similar plots are presented in Fig. 8 for an axigluon mass of $m_A = 5$ TeV, where now the generated asymmetry becomes positive due to the larger axigluon mass. In the former case the process is dominated by contributions with $\hat{s} > m_A^2$, in the latter case with $\hat{s} < m_A^2$, which implies a change in the sign of the axigluon propagator.
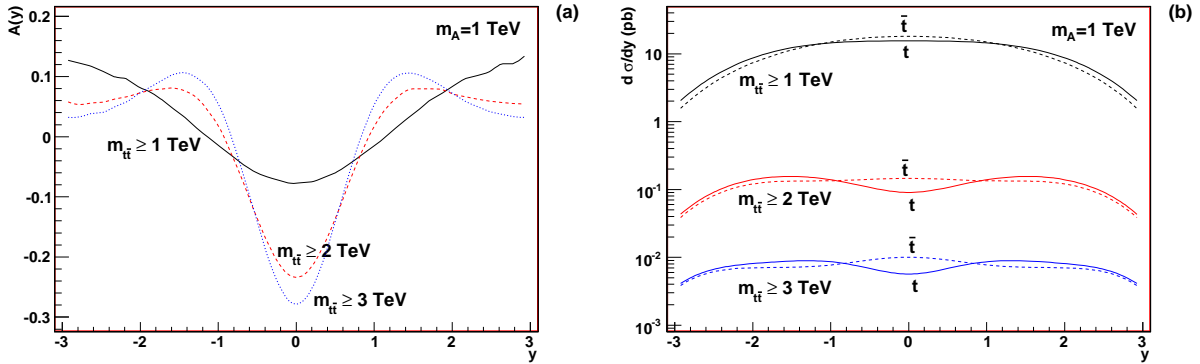

Figure 7: (a) Differential top quark charge asymmetry at LHC generated by the exchange of a massive axigluon with $m_A = 1$ TeV for samples with invariant top-antitop quark masses larger than 1, 2 and 3 TeV respectively. (b) Corresponding rapidity distributions of top quarks (solid) and antitop quarks (dashed). Factorization and renormalization scales are set to $\mu = m_t$.

In order to quantify the difference in the rapidity distribution globally we define a new charge asymmetry where only the the central region is taken into account:

$$A_C(y_C) = \frac{\sigma_t(|y| \leq y_C) - \sigma_{\bar{t}}(|y| \leq y_C)}{\sigma_t(|y| \leq y_C) + \sigma_{\bar{t}}(|y| \leq y_C)} \,. \tag{9}$$
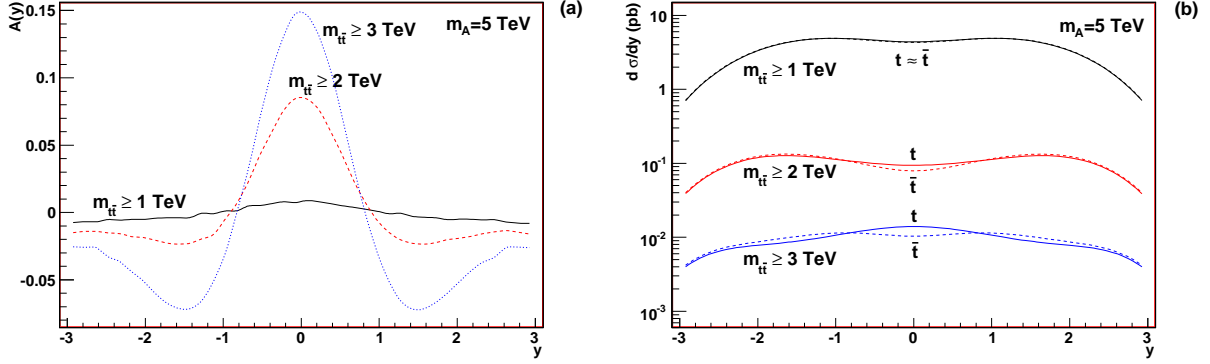
8

Figure 8: (a) Differential top quark charge asymmetry at LHC generated by the exchange of a massive axigluon with $m_A = 5$ TeV for samples with invariant top-antitop quark masses larger than 1, 2 and 3 TeV respectively. (b) Corresponding rapidity distributions of top quarks (solid) and antitop quarks (dashed). Factorization and renormalization scales are set to $\mu = m_t$.

Notice that $A_C(y_C)$ vanishes if the whole rapidity spectrum is integrated. Looking into Figs. 7(a) and 8(a) we expect that the maximum is reached at about $y_C = 1$. We thus report in Table 2 the values of the central asymmetry, integrated up to $y_C = 1$ for different values of the axigluon mass and for different values of the cut in the top-antitop invariant mass. The single inclusive top quark cross section in the central region is also listed (the corresponding antitop quark cross section can be deduced from the asymmetry). We also give in Table 2 the value of the QCD asymmetry in the central region, and in Fig. 9 the corresponding differential charge asymmetry. The central QCD charge asymmetry is never larger than 2%, and the reduction of the asymmetry for invariant masses above 2 TeV is due to a larger contribution of the flavour excitation processes that partly compensates the asymmetry generated by the $q\bar{q}$ events.

With 10 fb^{-1} integrated luminosity about 2000-2600 top quark events with $m_{t\bar{t}} \geq 2$ TeV are expected to be produced at LHC in the central region ($y_C = 1$), and a central charge asymmetry of about -2% is predicted from QCD alone. For $m_A = 5$ TeV the axigluon-induced asymmetry amounts to $+3\%$. For the same axigluon mass the total cross-section for $m_{t\bar{t}} \geq 4.5$ TeV is only 0.013 pb, one order of magnitude smaller than the central cross section for $m_{t\bar{t}} \geq 2$ TeV and $y_C = 1$. It is thus clear that even at LHC where no forward–backward asymmetry is generated, the central charge asymmetry can be used to probe larger axigluon masses than the top-antitop invariant mass spectrum [11, 12].

5 Summary

We have updated our previous analysis of the forward–backward and the charge asymmetry in top quark production at hadron colliders. We have also proposed a new observable , the pair asymmetry, where the effect at the Tevatron is enhanced by about a factor 1.5. Top quark production at the LHC is obviously forward–backward symmetric. Restricting the sample to events with large invariant $t\bar{t}$ mass and to t and $\bar{t}$ final states with rapidity below one a difference of $1 - 2\%$ in t versus $\bar{t}$ production cross section is observed.

9

		QCD	$m_A = 1$ TeV	$m_A = 2$ TeV	$m_A = 5$ TeV
$\sqrt{\hat{s}} \geq 1$ TeV	$A_C(y_C = 1)$	$-0.0086(4)$	$-0.055(4)$	$0.025(3)$	$0.002(1)$
	$\sigma_t(\lvert y \rvert \leq 1)$	$9.7(2.7)$ pb	$34(4)$ pb	$15(2)$ pb	$11(2)$ pb
$\sqrt{\hat{s}} \geq 2$ TeV	$A_C(y_C = 1)$	$-0.0207(14)$	$-0.10(2)$	$-0.048(5)$	$0.031(9)$
	$\sigma_t(\lvert y \rvert \leq 1)$	$0.19(6)$ pb	$0.28(8)$ pb	$1.7(2)$ pb	$0.26(7)$ pb
$\sqrt{\hat{s}} \geq 3$ TeV	$A_C(y_C = 1)$	$-0.0151(7)$	$-0.10(3)$	$-0.11(2)$	$0.057(13)$
	$\sigma_t(\lvert y \rvert \leq 1)$	$0.011(4)$ pb	$0.019(6)$ pb	$0.024(7)$ pb	$0.031(8)$ pb

Table 2: Central charge asymmetry at LHC, $\sqrt{s} = 14$ TeV, for different values of the axigluon mass and different cuts in the invariant mass of the top-antitop pair. We also present the LO prediction for the top quark cross section in the central region.
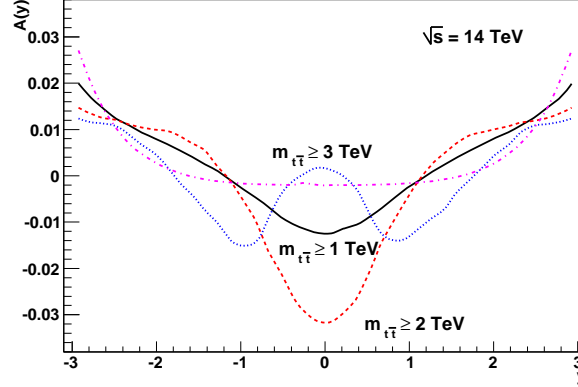

Figure 9: Differential QCD charge asymmetry at LHC for top-antitop quark invariant masses larger than $2m_t$ (dotted-dashed), 1 TeV (solid), 2 TeV (dashed), and 3 TeV (dotted) respectively. Factorization and renormalization scales are set to $\mu = m_t$.

The analysis has been extended to the asymmetry induced by axigluon contributions to the amplitude, which is the most important manifestation of such an exotic object. Already present preliminary results on the charge asymmetry from the Tevatron lead to an limit on the axigluon mass of around 1.2 TeV. The analysis has been extended to the LHC. Restricting the event sample to regions of large $t\bar{t}$ mass with $q\bar{q}$ induced production, large axigluon masses can be explored.

Acknowledgements

A Born cross-section

The Born cross-section for $q\bar{q}$ fusion in the presence of an axigluon vector resonance reads

$$\frac{d\sigma^{q\bar{q}\to t\bar{t}}}{d\cos\hat{\theta}} = \alpha_s^2\,\frac{T_F C_F}{N_C}\,\frac{\pi\beta}{2\hat{s}}\left(1 + c^2 + 4m^2 + \frac{4\,c\,\hat{s}(\hat{s}-m_A^2)+\hat{s}^2\,(\beta^2+c^2)}{(\hat{s}-m_A^2)^2+m_A^2\Gamma_A^2}\right)\,, \tag{10}$$

where $\hat{\theta}$ is the polar angle of the top quark with respect to the incoming quark in the center of mass rest frame, $\hat{s}$ is the squared partonic invariant mass, $T_F = 1/2$, $N_C = 3$ and $C_F = 4/3$ are the color factors, $\beta = \sqrt{1-4m^2}$ is the velocity of the top quark, with $m = m_t/\sqrt{\hat{s}}$, and $c = \beta\cos\hat{\theta}$. Our result in Eq. (10) agrees with the expression of Ref. [12], and therefore confirms the disagreement with respect to Eq.(2) of Ref. [13]. The term odd in c in Eq. (10) is due to the interference between the gluon and the axigluon amplitudes. The decay width of the axigluon is given by [11, 12]:

$$\Gamma_A \equiv \sum_q \Gamma(A \to q\bar{q}) \approx \frac{\alpha_s\,m_A\,T_F}{3}\left[5 + \left(1 - \frac{4m_t^2}{m_A^2}\right)^{3/2}\right]\,. \tag{11}$$

Because of parity there are no gluon-axigluon vertices with an odd number of axigluons [11], and therefore the Born gluon-gluon fusion cross-section is the same as in the SM [2]:

$$\frac{d\sigma^{gg\to t\bar{t}}}{d\cos\hat{\theta}} = \alpha_s^2\,\frac{\pi\beta}{2\hat{s}}\left(\frac{1}{N_C(1-c^2)} - \frac{T_F}{2C_F}\right)\left(1 + c^2 + 8m^2 - \frac{32m^4}{1-c^2}\right)\,. \tag{12}$$

References

[1] F. Gianotti and M. L. Mangano, arXiv:hep-ph/0504221.

[2] J. H. Kühn and G. Rodrigo, Phys. Rev. D **59**, 054017 (1999) [arXiv:hep-ph/9807420]; Phys. Rev. Lett. **81**, 49 (1998) [arXiv:hep-ph/9802268].

[3] F. Halzen, P. Hoyer and C. S. Kim, Phys. Lett. B **195** (1987) 74.

[4] S. Catani, D. de Florian, G. Rodrigo and W. Vogelsang, Phys. Rev. Lett. **93** (2004) 152003 [arXiv:hep-ph/0404240].

[5] S. Dittmaier, P. Uwer and S. Weinzierl, Phys. Rev. Lett. **98**, 262002 (2007) [arXiv:hep-ph/0703120].

[6] M. T. Bowen, S. D. Ellis and D. Rainwater, Phys. Rev. D **73**, 014008 (2006) [arXiv:hep-ph/0509267].

[7] J. Weinelt, Masters thesis, Universität Karlsruhe, FERMILAB-MASTERS-2006-05; IEKP-KA-2006-21.

[8] D. Hirschbuehl, Ph.D. Thesis, Universität Karlsruhe, FERMILAB-THESIS-2005-80.

[9] T. A. Schwarz, Ph.D. Thesis, University of Michigan, FERMILAB-THESIS-2006-51, UMI-32-38081.

[10] J. C. Pati and A. Salam, Phys. Lett. B **58** (1975) 333. L. J. Hall and A. E. Nelson, Phys. Lett. B **153** (1985) 430. P. H. Frampton and S. L. Glashow, Phys. Lett. B **190** (1987) 157; Phys. Rev. Lett. **58** (1987) 2168.

[11] J. Bagger, C. Schmidt and S. King, Phys. Rev. D **37** (1988) 1188.

[12] D. Choudhury, R. M. Godbole, R. K. Singh and K. Wagh, arXiv:0705.1499 [hep-ph].

[13] L. M. Sehgal and M. Wanninger, Phys. Lett. B **200** (1988) 211.

[14] S. Dimopoulos, Nucl. Phys. B **168** (1980) 69. J. Preskill, Nucl. Phys. B **177** (1981) 21.

[15] M. P. Giordani [CDF and D0 Collaborations], Eur. Phys. J. C **33** (2004) S785.

[16] F. Abe *et al.* [CDF Collaboration], Phys. Rev. D **55**, 5263 (1997) [arXiv:hep-ex/9702004].

[17] T. G. Rizzo, Phys. Lett. B **197** (1987) 273.

[18] F. Cuypers and P. H. Frampton, Phys. Rev. Lett. **60** (1988) 1237. M. A. Doncheski, H. Grotch and R. W. Robinett, Phys. Rev. D **38** (1988) 412; Phys. Lett. B **206** (1988) 137.

[19] E. D. Carlson, S. L. Glashow and E. E. Jenkins, Phys. Lett. B **202** (1988) 281.

[20] M. A. Doncheski and R. W. Robinett, Phys. Rev. D **58** (1998) 097702 [arXiv:hep-ph/9804226]; Phys. Lett. B **412** (1997) 91 [arXiv:hep-ph/9706490].

[21] The Tevatron Electroweak Working Group, arXiv:hep-ex/0703034.

[22] A. D. Martin, W. J. Stirling and R. S. Thorne, Phys. Lett. B **636** (2006) 259 [arXiv:hep-ph/0603143].

[23] R. Bonciani, S. Catani, M. L. Mangano and P. Nason, Nucl. Phys. B **529** (1998) 424 [arXiv:hep-ph/9801375].